

Bentonite Clay and Waterglass Porous Monoliths Via the Sol-Gel Process

Luqman A. ADAMS*¹ Rafiu O. SHAIBU,¹ Reginald E. ESSIEN,² and Aderemi OKI³

¹*Department of Chemistry, Faculty of Science, University of Lagos, Nigeria*

²*Department of Chemical Sciences, Bells University of Technology, Ota, Ogun State, Nigeria*

³*Department of Chemistry, Prairie View A & M University, Texas, USA*

Abstract

Porous silicate glass monoliths were obtained from two inexpensive precursors; sodium metasilicate (waterglass) (Na_2SiO_3) (SMS) and bentonite clay (BTC) using the sol gel synthesis. The optimal gelation mole ratio for SMS was ($\text{Na}_2\text{SiO}_3 : \text{H}_2\text{O} : \text{H}_2\text{SO}_4 : \text{C}_2\text{H}_5\text{OH}$) of (1 : 13.54 : 0.5 : 1.68); while gelation for BTC was ($\text{BTC} : \text{H}_2\text{O} : \text{H}_2\text{SO}_4 : \text{C}_2\text{H}_5\text{OH}$) of (1 : 13.54 : 1.0 : 1.68). The gels obtained were initially washed with deionised water to free the (Si-O-Si) framework from Na_2SO_4 as by-product of the hydrolysis, followed by aging, drying at low temperature before finally sintering at 600°C to give the monoliths. The bulk density of the monoliths obtained were determined, and further characterized using Fourier transform infra red (FTIR) spectroscopy, X-ray diffraction (XRD) spectroscopy, Atomic absorption spectroscopy (AAS), and Scanning electron microscopy (SEM). The monoliths show macroporous structure with pore size ranging from 150 – 250 nm, and can be further tailored to give scaffolds for bone tissue repair.

Key words : Sol-gel, Bioceramics, Monolith, Sodium metasilicate, Bentonite clay

Introduction

Sol-gel silica glasses have received considerable attention in recent times as convenient routes to preparation of bioceramics. Such bioactive glasses have been reported to stimulate the regeneration of compromised bone tissues.^(1,2) An enormous array of biomaterials proposed as ideal scaffolds have emerged.⁽³⁾ Calcium phosphate ceramics and bioactive glasses used as substitutes bond to bone whereby they enhance bone tissue formation,⁽⁴⁾ ultimately making silica-based glasses one of the most interesting bioceramics during the last 40 years.^(5,6)

Generally sol-gel process uses alkoxysilanes precursors, such as tetraethyl orthosilicate (TEOS) and tetramethyl orthosilicate (TMOS) as silica sources in the pathway to bioactive glass-ceramics.⁽⁷⁾ The chemistry of silicon alkoxide gelation is very straightforward, with the side products – alcohol and water being removable by evaporation. Alkoxides however have their drawbacks, hazardous on inhalation, and expensive to prepare over several steps.⁽⁸⁾ Notwithstanding, the sol-gel process⁽⁹⁾ presents several processing advantages, mainly because of the versatility, purity, homogeneity and the possibility to modify the material parameters⁽¹⁰⁾, such as higher surface area and porosity which are critical for bioactivity.^(11,12)

The minimum pore diameter required for bone in-growth and angiogenesis into a scaffold is considered to be $100\ \mu\text{m}$.⁽¹³⁾ Previous in vitro work has suggested that the ideal pore diameter for bone ingrowth is between $300\text{-}400\ \mu\text{m}$.⁽¹⁴⁾

Unlike silicon alkoxides, sodium silicates are slightly basic, and are hydrolysed to the sol catalysed by acid (such as hydrochloric or sulfuric acid) to form silanol (Si-OH) groups. However, the gels formed for example via the sulphuric acid reaction will contain both Na^+ and SO_4^{2-} ions that can affect the gel framework. Hydrophobic silica aerogels have been prepared from waterglass through hydrolysis, gelation and water washing of the gel to remove Na^+ ions.⁽⁸⁾ Crack free aerogel was prepared via solvent exchange and surface modification of the wet gels.⁽¹⁵⁾

In this work, we have utilized waterglass (sodium metasilicate) and bentonite clay as precursors to porous silicate glass monoliths via acid mediated sol-gel hydrolysis, gelation, water washing of the gel, drying and sintering to afford the monolith. This work shows a facile and inexpensive route to porous silicate glass monolith using bentonite clay.

Materials and Experimental Procedures

Materials

The chemicals used were sodium metasilicate (Na_2SiO_3), (SMS) (Merck) had the composition SiO_2 24.9 and Na_2O 20.9 wt% respectively, bentonite clay (BTC) was obtained locally, sulphuric acid (H_2SO_4), (Fluka, Germany), ethanol ($\text{C}_2\text{H}_5\text{OH}$), (Merck) and methanol (CH_3OH), (Merck). The reagents were used as purchased without further purification.

Preparation of Silica Monolith from Sodium Metasilicate (SMS)

Sodium metasilicate (5.0 g, 41.0 mmole) was stirred in distilled water (10.0 ml) followed by ethanol (4.0 ml) to give a clear solution. Thereafter, 10.0 ml of 2M H_2SO_4 was added dropwise to the mixture under magnetic stirring at room temperature for about 2h to form a gel. Deionised water was added successively to wash and remove sodium sulphate. Complete removal of sodium ions was indicated by absence of white precipitate when the final filtrate was tested with dilute lead (II) ethanoate solution. Thereafter, the gel was cast into plastic mould and methanol added to exchange the water in the gel over 24 hours. After decantation of the solvent, the gel was dried at ambient conditions for 24 hours, followed by drying at 50°C for 1 hour and at 70°C for one day. The gel was finally calcined at 600°C for 2 hours to obtain the monolith.

Preparation of Silica Monolith from Bentonite Clay (BTC)

Bentonite clay (10.0 g) was refluxed in 1M NaOH solution (200.0 ml) for 2 hours. The filtrate obtained was evaporated to dryness to give as residue sodium metasilicate (5.0g). The basic sodium metasilicate was dissolved in distilled water (10.0 ml). The solution was hydrolysed with 2M H_2SO_4 (20.0 ml) and subsequently treated the same way as in 2.2 above to afford the bentonite clay silicate glass monolith.

Characterization

The bulk density of the monoliths was calculated based on a known volume of monolith and dividing it by its mass (measured by a microbalance, 10^{-5} precision). The volume was determined using immersion technique in a known

quantity of water. X-ray diffraction (XRD) analysis was carried out in the 2θ range of $5-120^\circ$ using Xpert PRO PANalytical diffractometer employing $\text{CuK}\alpha$ radiation (0.154060 nm) source operated at 40kV and 40mA. Fourier transform infrared spectroscopy (FTIR) studies were carried out using Buck Scientific 500 Infra red spectrophotometer with KBr as reference in the wave number range of $600-4000\text{ cm}^{-1}$. Atomic absorption spectroscopy (AAS) Perkin Elmer A Analyst 200 was used to determine residual amount of sodium ions (Na^+) present in the monolith. Morphological characterization of the samples regarding the particles and pore sizes distribution were performed using a SEM (EVO/MA10) at an accelerating voltage of 10kV.

Results and Discussion

Hydrolysis and Gelation

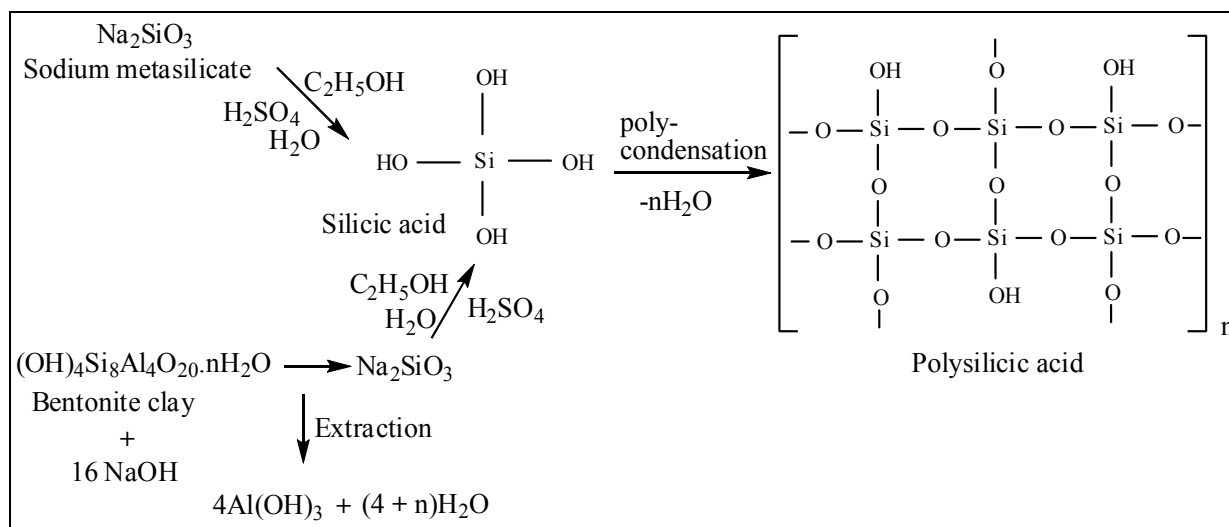
The precursor sodium metasilicate and bentonite clay are shown in Figures 1(a-b). Acidic hydrolysis of sodium metasilicate (Na_2SiO_3) gives silicic acid⁽¹⁶⁾ in solution. Sodium hydroxide is reacted with bentonite clay to initially afford sodium metasilicate in a strongly basic medium. The water glass obtained from the basic reaction is similarly hydrolysed to silicic acid which undergoes condensation to disilicic acid and further reaction to a polycondensed hydrogel⁽¹⁶⁾ as shown in Figure 2. Thereafter, the gel obtained from both precursor compounds were subjected to multiple washings⁽⁸⁾ with deionised water as shown in Figure 3 in order to free the gel of sodium sulphate formed during hydrolysis.

The 3-D framework of the silicate glass continues to grow and becomes more rigid by contracting and expelling liquid water present inside the pores.⁽¹⁷⁾ The hydrogel becomes less porous, harder and cannot be compressed (18) further now as a monolith. Alcohol (methanol or ethanol) can be used to replace water impregnating the gel in order to improve the quality and to facilitate the non-destructive drying of the gel.⁽¹⁸⁾



(a)

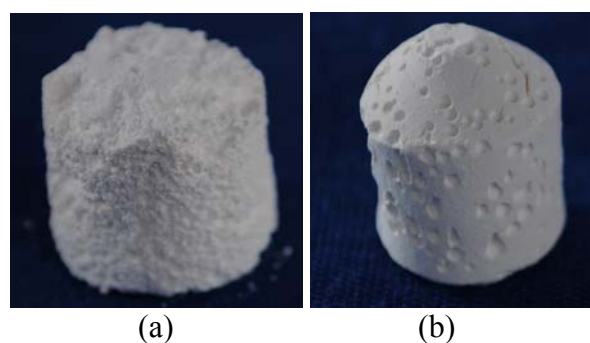
(b)

Figure 1. (a) Sodium metasilicate, and (b) Bentonite clay.**Figure 2.** Hydrolysis and polycondensation of sodium metasilicate and bentonite clay.**Figure 3.** Washing of gels in deionized water.

The efficiency of deionised water washings to free the gel from sodium sulphate was monitored by atomic absorption spectroscopy (AAS) analysis of the monolith obtained after drying. The result indicated that Na^+ decreased from 36.5% (on the basis of stoichiometry)⁽⁸⁾ to 1.81% in the SMS-based monolith and 2.5% for the BTC-based monolith respectively.

Bulk Density of Monoliths

The silicate glass monolith obtained from (SMS) Figure 4a and (BTC) Figure 4b after calcination were found to have bulk density of 0.84 and 0.77 g cm^{-3} respectively. The difference may be due to better packing of the 3-D framework in the SMS monolith as a result of more efficient removal of the interfering Na^+ from successive deionized water washings of the gels.

**Figure 4.** Monolith from (a) sodium metasilicate, and (b) bentonite clay.

FTIR Characterisation of the Monoliths

The FTIR spectra obtained for the SMS and BTC based monoliths respectively are characterized by a broad band centred around 3400 cm^{-1} and a smaller signal around 1600 cm^{-1} that corresponds to O-H absorption band⁽¹⁵⁾ as shown in Figure 5a and 5b. Furthermore, a diagnostic Si-O-Si asymmetric stretching vibration is centred on 1132 cm^{-1} ^(19,20), the absorption signal at 920 cm^{-1} is assigned to the stretching vibration of silanol groups on the surface of the amorphous solid.⁽²¹⁾

XRD Characterisation of the Monoliths

X-ray diffraction technique was employed as a versatile, non-destructive technique that reveals detailed information about the chemical composition and crystallographic structure of

natural and manufactured materials. XRD analysis of the calcined monoliths for SMS and BTC are shown in Figure 6a and 6b respectively. The spectra for both samples indicated presence of SiO₂ networks which had amorphous structure, with a peak observed at $2\theta=22^\circ$.⁽²²⁾

SEM Characterisation of the Monoliths

Pore size distribution analysis for the SMS and BTC based monoliths were analysed using SEM as shown in Figure 7a and 7b respectively. Figure 7a for the SMS monolith appears to indicate more ordered arrangement of the particles compared to the BTC based monolith in Figure 7b. Generally, the SMS monolith shows pore size range about 188 – 250 nm, while for the BTC monolith pore sizes is in the range of 150 – 200 nm. Both porous glass monolith fall in the macroporous materials range. Large surface area micro-porosity is a property essential in bioceramics for protein cell adhesion, cell migration and osteointegration.^(13, 23-26)

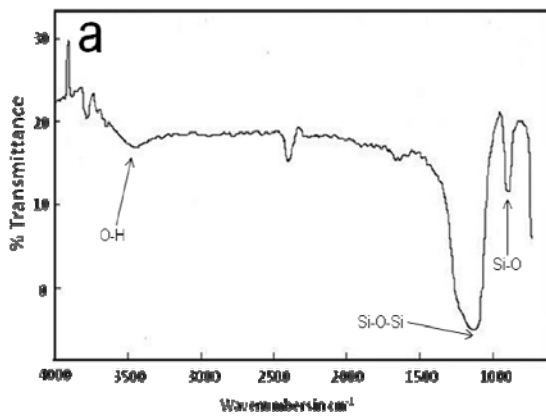


Figure 5a. FTIR spectra of SMS monolith.

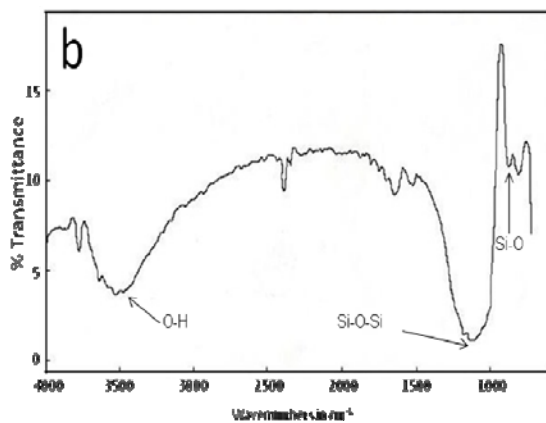


Figure 5b. FTIR spectra of BTC monolith.

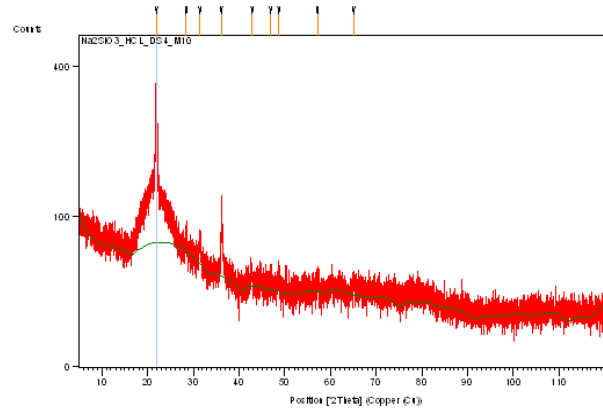


Figure 6a. XRD patterns of the SMS based monolith.

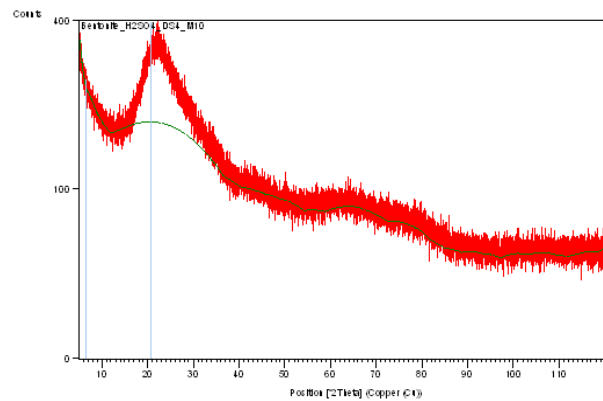
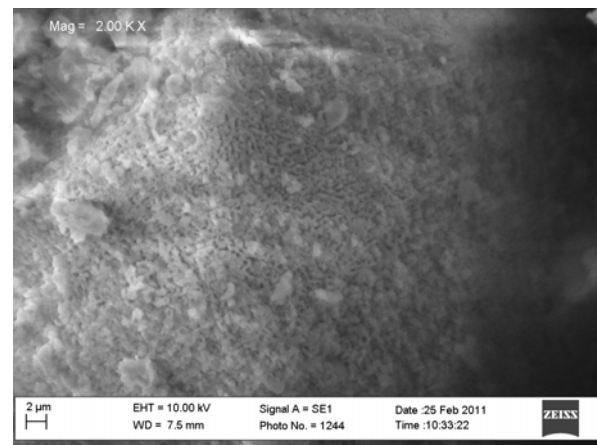
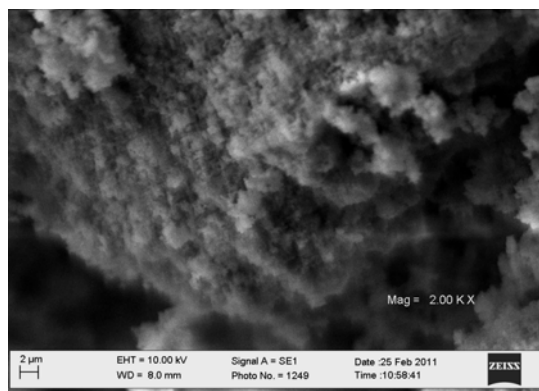


Figure 6b. XRD patterns of the BTC-based monolith.



(a)

Figure 7a. SEM micrographs showing the surface morphology of the monolith from SMS.



(b)

Figure 7b. SEM micrographs showing the surface morphology of the monolith from BTC.

Conclusion

Low temperature silicate glass monoliths were prepared from two inexpensive precursors; sodium metasilicate and bentonite clay. After acid hydrolysis and polycondensation of the gels, repeated washings of the gels with deionised water facilitate the removal of contaminating sodium sulphate in the gel framework. SEM analysis revealed the poor average pore size obtained for the monolith when compared to ideal pore diameter required for bone ingrowth which is between 300-400 μm .

XRD characterisation revealed an amorphous state for the monoliths, while the FTIR analysis indicated characteristic absorption bands for Si-O-Si and silanol groups in the framework. This study is ongoing as we work to obtain materials with desirable properties for use as bioceramics in *in vivo* bone therapy by exploiting the abundant inexpensive clays and sodium metasilicate as precursor compounds relative to the alkoxy silanes.

Acknowledgements

The authors are grateful to the CIDA Research Center for the SEM analysis, and Bells University, Ota for Financial Assistance to R. E. Essien.

References

1. Jones, J. R., Gentleman, E. and Polak, J. (2007). Bioactive glass scaffolds for bone Regeneration. *Elements* **3(6)** : 393-399.

2. Hench, L. L. and Polak, J. M. (2002). Third-Generation Biomedical Materials Science **8(295)** : 1014-1017.
3. El-Ghannam, A. (2005). Bone reconstruction: from bioceramics to tissue engineering. *Expert Rev.Med. Dev.* **2(1)** : 87-101.
4. Arinzeh, T. L., Tran, T., Mcalary, J. and Daculsi, G. (2005). A comparative study of biphasic calcium phosphate ceramics for human mesenchymal stem-cell-induced bone formation. *Biomaterials* **26(17)** : 3631-3638.
5. Hamadouche, M., Meunier, A., Greenspan, D. C., Blanchat, C., Zhong, J. P., La Torre, G. P. and Sedel, L. (2001). Long-term in vivo bioactivity and degradability of bulk sol-gel bioactive glasses. *J. Biomed. Mater. Res* **54(4)** : 560–566.
6. Arcos, D. and Vallet-Regi, M. (2010). Sol-Gel Silica-based biomaterials and Bone tissue regeneration. *Acta Biomater.* **6** : 2874-2888.
7. Nayak, J. P., Kumar, S. and Bera, J. (2010). Sol-gel synthesis of Bioglass-Ceramics Using rice Ash as a source for silica and its characterization. *J. Non-Cryst. Solids* **356** : 1447-1451.
8. Bangi, U.K., Rao, A.V. and Rao, A.P. (2008). A New Route for Preparation of Sodium-Silicate-Based hydrophobic silica aerogels via Ambient-Pressure drying. *Sci. Technol. Adv. Mater.* **9** : 1-10.
9. Hench, L. L. and West, J. K. (1990). The sol-gel process. *Chem. Rev.* **90(1)** : 33–72.
10. Chen, Q., Miyata, N., Kokubo, T. and Nakamura, T. (2000). Bioactivity and mechanical properties of PDMS-modified CaO–SiO₂–TiO₂ hybrids prepared by sol-gel process. *J. Biomed. Mater. Res.* **51(4)** : 605–611
11. Sepulveda, P., Jones, J.R. and Hench, L.L. (2005). Bioactive Sol-gel foams for tissue repair. *J. Biomed. Mater. Res.* **59** : 340-348.

12. Best, S. M., Porter, A. E., Thian, E. S. Huang, J. (2008). Bioceramics: Past, present and for the future. *J. Eur. Ceram. Soc.* **28(7)** : 1319-1327.
13. Karageorgiou, V. and Kaplan D. (2005). Porosity of 3D Biomaterial scaffolds and osteogenesis. *Biomaterials* **26(27)** : 5474-5491.
14. Tsuruga, E., Tahita H., Itoh H, Wakisaka, Y. and Kuboki Y. (1997). Pore size of porous hydroxyapatite as the Cell-Substratum controls BMP-Induced osteogenesis. *J. Biochem.* **121(2)** : 317-324.
15. Lee, C. J., Kim, G. S. and Hyun, S. H. (2002). Synthesis of silica aerogels from waterglass via new modified ambient drying, *J. Mater. Sci.* **37(11)** : 2237-2241.
16. Wang, H., Zhong, W., Du, Q., Yang, Y., Okamoto, H. and Inoue, S. (2003). Novel polyimide/silica nanohybrids from water glass. *Polym.Bull.* **51** : 63-68.
17. Hwang, S-W., Kim, T-Y. and Hyun, S-H. (2010). Effect of surface modification conditions on the synthesis of mesoporous crack-free silica aerogel monoliths from waterglass via ambient-drying. *Microporous Mesoporous Mater.* **130(1)** : 295-302.
18. Besbes, M., Fakhfakh, N. and Benzina, M. (2009). Characterization of silica gel prepared by using Sol-gel process, physics. *Procedia* **2(3)** : 1087-1095.
19. Mansur, H. S., Orefice, R. L. and Mansur, A.A.P. (2004). Characterization of Poly(vinyl alcohol)/Poly(ethylene glycol) hydrogels and PVA-Derived Hybrids by Small-Angle scattering and FTIR spectroscopy. *Polymer* **45(21)** : 7193 - 7202.
20. Almeida, R. and Pantano, G. (1990). Structural investigation of silica gel films by infrared spectroscopy. *J. Appl. Phys.* **68** : 4225-4230.
21. Lenza, R.F.S. and Vasconcelos, W.L. (2001). Preparation of silica by Sol-Gel method using formamide. *Mater. Res.* **4(3)** : 189-194.
22. Sooksaen, P., Suttiruengwong, S., Oniem, K., Ngamlamiad, K. And Atireklapwarodom, J. (2008). Fabrication of porous bioactive Glass-Ceramics via decomposition of natural fibres. *J. Met. Mater. Miner.* **18(2)** : 85-91.
23. Vitale-Brovarone, C., Miola, M., Balagna, C. and Verne, E. (2008). Scaffolds with antibacterial properties for bone grafting. *Chem. Eng. J.* **137** : 129-136.
24. Smith, I.O., Ren, F., Baumann, M.J. and Case, E.D. (2006). Laser scanning microscopy as a tool for imaging cancellous bone. *J. Biomed. Mater. Res. B Appl. Biomater.* **79** : 185- 192.
25. Woodard, M. B., Hilldore, A. J., Lan, S. K., Park, C. J., Morgan, A. W., Eurell, J. A., Clark, S. G., Wheeler, M. B., Jamison, R. D. and Wagona- Johnson, A. J. (2007). The Mechanical properties and osteoconductivity of hydroxyapatite bone scaffold with Multi-Scale porosity. *Biomaterials* **28(1)** : 45-54.
26. Vitale-Brovarone, C., Baino, F. and Verne, E. (2009). High strength bioactive Glass-Ceramic scaffolds for bone regeneration. *J. Mater. Sci. Mater. Med.* **20** : 643-653.